JOURNAL OF MATERIALS SCIENCE 14 (1979) 653–662

The fatigue properties of cross-plied boron 6061 aluminium

M. K. WHITE, M. A. WRIGHT
University of Tennessee Space Institute, Tullahoma, Tennessee 37388, USA

The mechanical properties of 0/90° and 0/90/± 45° boron–aluminium laminates have been examined at room temperature, 200 and 300° C. The increase in test temperature resulted in decreases in both the tensile and fatigue properties. Relatively constant critical stress intensity values were obtained from centre-notched static tensile specimens, indicating high notch sensitivity. Smaller values were obtained from specimens tested at elevated temperatures.

The tension–compression ($R = -1$) fatigue behaviour of unnotched specimens cut from either material indicated 10^7 cycle endurance limits of about 255 MPa (37×10^3 psi) and endurance ratios of 0.3 to 0.4. Microscopic examination of failed specimens detected the presence of off-axis fibre splitting and multiple cracks that were distributed throughout the matrix. Fractographic observations indicated that the fatigue crack had propagated completely through the matrix before final failure of the fibres occurred.

Notched specimens failed by fracture at the fatigue extended notch at approximately the same values of the critical stress intensity that had been determined statically. However, fatigue lives obtained from centre-notched specimens subjected to identical net section stresses indicated that the rate of propagation of the premachined notch was faster for specimens containing longer crack sizes only for crack length: specimen width ratios, $2a/w$, up to 0.4; thereafter, larger ratios yielded slower crack propagation rates.

1. Introduction

There have been a number of published papers in which the results of fatigue tests carried out on fibre-reinforced metal–matrix composites have been reported [1–4]. Some of the experiments involved bend tests, where the rate of degradation of the material stiffness was taken as some measure of the fatigue resistance. Tension–tension fatigue tests have also been carried out. It has been argued that the results indicated that the fatigue performance of unidirectionally reinforced fibre composites was generally significantly better than that of most conventional metals. It was further concluded that although the absolute value of the fatigue strength was dependent on the properties of the fibres, it was the matrix that controlled the fatigue fracture mechanism.

Boron-fibre-reinforced aluminium is mostly produced as relatively thin plates. Thus, specimens cut from this material are difficult to test in compression. The results that are presented in this paper attempt to rectify this deficiency, for they were obtained from cross-plied boron–aluminium specimens tested in fully reversed push–pull loading ($R = -1$). Support for the specimen was provided during the compression cycle by the use of antibuckling plates.

2. Experimental technique

Unnotched and centre-notched specimens were prepared from diffusion bonded 6061-aluminium alloy reinforced with boron fibres. Two materials were fabricated; type one contained fibres oriented parallel and perpendicular to the load axis, and type two contained additional fibres oriented in the 45° directions. Thirteen layers of boron fibres having a diameter of 0.145 mm (5.7×10^{-3} in.) were used to form 30 cm × 30 cm

(12 in. x 12 in.) panels nominally 2.54 mm (0.1 in.) thick containing approximately 47 vol % reinforcement. Individual specimens, 10.2 cm x 2.54 cm (4 in. x 1 in.) were cut from each panel using electric discharge machining (EDM) or a diamond wheel.

Centre notches 2.5, 5.1, 10.2 and 15.2 mm (0.1, 0.2, 0.4 and 0.6 in.) long were machined in some of the specimens by EDM. To avoid damage and subsequent failure within the gripped ends, aluminium tabs 3.8 cm x 2.5 cm (1.5 in. x 1 in.) were attached with an epoxy adhesive to the room temperature specimens, resulting in a 2.5 cm (1 in.) long gauge length. At elevated temperatures, abrasive screen cloth was used between the tabs and the specimen in order to improve the necessary stress transfer.

The static properties were obtained using an Instron screw driven tensile test machine operating at a cross-head displacement rate of 0.51 mm min^{-1} (0.02 in. min^{-1}). Constant load amplitude tension–compression ($R = -1$) testing was performed with an MTS servo-hydraulic machine operating at a frequency of 10 to 25 Hz sinusoidal. The frequency used for a given test was generally near the maximum capability of the machine at a given load amplitude. Antibuckling constraint was provided at room temperature by 2.5 cm (1 in.) thick clear plastic bars clamped across the specimen test section. Cracking of notched specimens was observed through these support bars. Both fatigue and static testing was performed at 200 and 300° C using steel supports containing heating elements. A thermocouple, contacting the specimen through a hole in one of the support bars, was used to measure and regulate the temperature. In order to reduce friction, teflon films were inserted between the specimen and the support at the lower temperatures. A combination of thin graphite shims and a high temperature lubricant was used at 300° C. Naturally, no observation of cracking was possible during the elevated temperature tests.

3. Results and discussion

Results from static tests carried out at room temperature indicated that the elastic modulus of both the 0/90° and 0/90/±45° material was 1.62×10^5 MPa (23.5×10^6 psi) up to a strain of 0.001. At this point, plastic flow of the matrix occurred and the respective modulus values decreased to 9.10×10^4 MPa (13.2×10^6 psi) and 8.34×10^4 MPa (12.1×10^6 psi). This decrease resulted from the resulted from the reduced relative load bearing ability of the off-axis layers. Both materials failed at strains of about 0.008.

At room temperature, a mean ultimate strength of 779 MPa (113×10^3 psi) was exhibited by the 0/90° material; the corresponding strength of the 0/90/±45° material was 655 MPa (95×10^3 psi). If

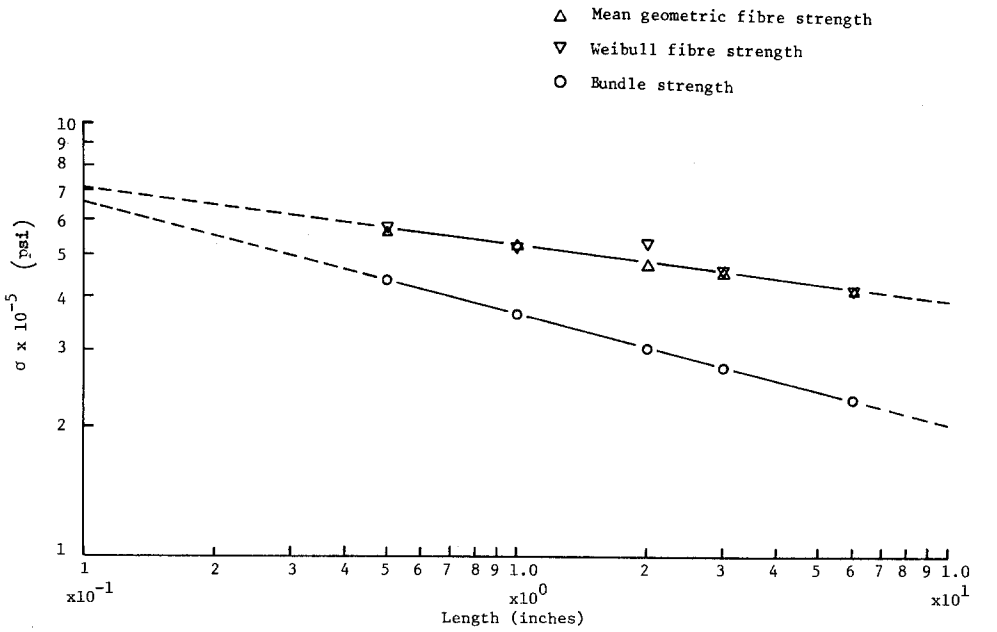

Figure 1 Experimental boron fibre strength data.

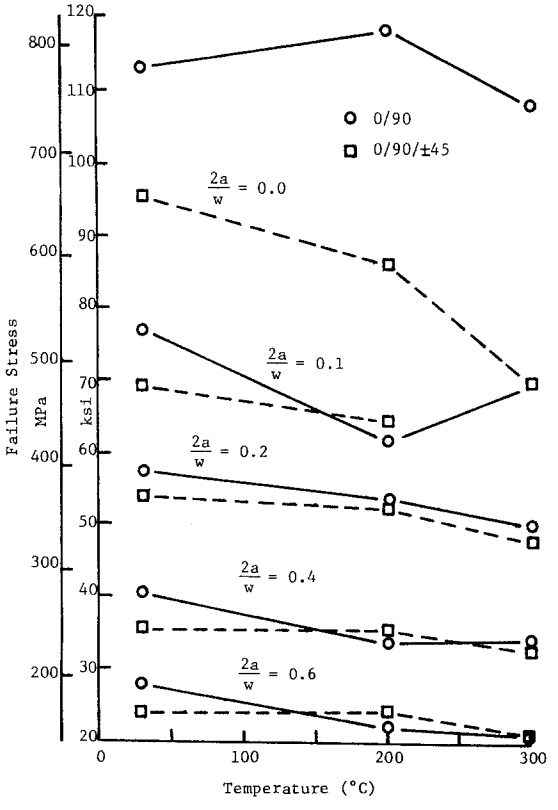

Figure 2 Effect of temperature on the static tensile strength of cross-plied boron–aluminium.

it is assumed that the 90° layers were not carrying a significant load when the composite failed, then the strength of the seven 0° layers present in the 0/90° material was 1448 MPa (210 × 10^3 psi). This value is almost identical to the commonly reported strengths of unidirectional 47 vol% boron–aluminium [5–7]. Assuming this strength was also characteristic of the five 0° layers in the 0/90/±45° material, then the four 45° layers contributed only about 97 MPa (14 × 10^3 psi) to the strength of the composite.

The effective strength of the fibres in a composite is given by the expression:

$$\sigma_f = (\sigma_c - (1 - v_f)\sigma_m)/v_f, \qquad (1)$$

where σ_c is the composite strength, v_f is the fibre volume fraction and σ_m is the tensile stress in the matrix at composite failure.

If 69 MPa (10 × 10^3 psi) is taken for a realistic value of σ_m, then substituting a value of 1448 MPa (210 × 10^3 psi) for σ_c in Equation 1 indicates that the strength of the bundle of fibres within each 0° layer, σ_f, is equal to 3006 MPa (436 × 10^3 psi) for material containing a 0.47 volume fraction of fibres. As has been discussed in the literature, the strength of a bundle of boron fibres is determined from the Weibull relationship [8, 9]

$$\sigma_B = \sigma_0 [(L/D)\omega e]^{1/\omega} \qquad (2)$$

where σ_0 is the constant related to the maximum strength of the fibre, ω describes the variation of individual fibre strength, and D is the diameter of fibres of length equal to L.

The mean strengths of fifty fibres that were extracted from the test specimens used in this investigation are shown as individual points in Fig. 1. The corresponding values of the Weibull constants that were deduced from these data are equal to 3.9 and 1.75 × 10^4 MPa (2.54 × 10^6 psi) for ω and σ_0, respectively. Values of the strength expected from different length fibre bundles were calculated using Equation 2 and these are also indicated in Fig. 1. It is to be noted that the strength of a 1 in. bundle is expected to be 2537 MPa (368 × 10^3 psi). Thus, since the strength of the fibres when present in the composite is greater than the expected strength of a bundle of fibres of the same length, it can be concluded that the boron fibres reinforced the aluminium matrix synergistically. This effect has been discussed in previous work [9].

The static strengths exhibited by both the notched and unnotched specimens when tested at room temperature, 200 and 300° C are shown in Fig. 2. In general, the strengths were lower at higher temperatures; however, the unnotched 0/90/±45° material exhibited the greatest temperature sensitivity. This effect is not unexpected, since the properties of the matrix dominate the response of the 45° layers and hence, the total response of the composite is more matrix dependent. The shear strength of the matrix is particularly important. For instance, if the matrix shear strength were reduced to zero then the effective strength of the 0° fibres present in the composite would decrease from the value calculated from the room temperature strength of the composite, i.e. 3006 MPa (436 × 10^3 psi), to the value expected from a simple 1 in. long bundle, i.e. 2537 MPa (368 × 10^3 psi). The corresponding strength of the unnotched composites would be about 641 MPa (93 × 10^3 psi) and 455 MPa (66 × 10^3 psi) for the 0/90° and 0/90/±45° materials, respectively. As can be observed, these expected values are reasonably close to those observed at the higher temperature.

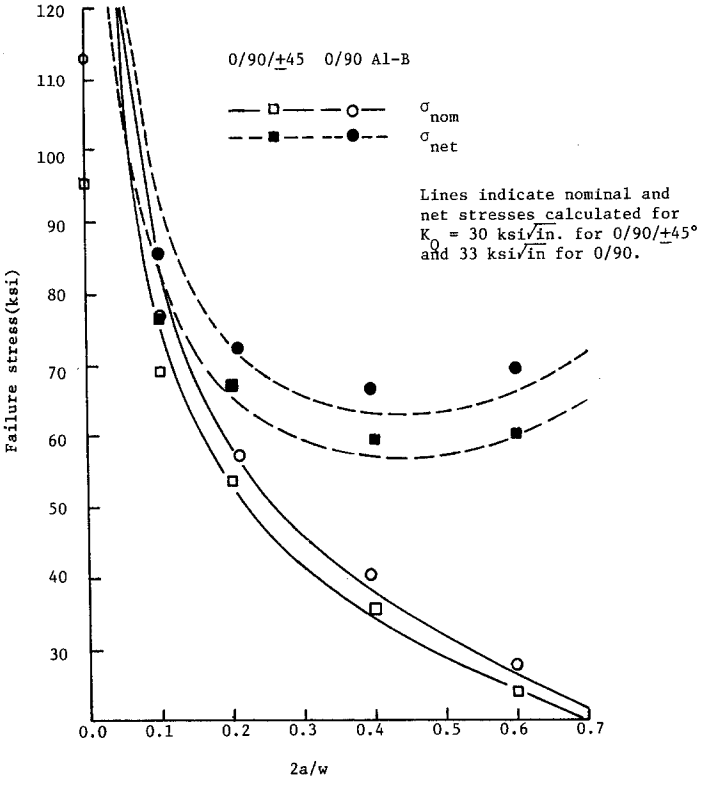

Figure 3 Effect of notch length on static room temperature strength of cross-plied boron–aluminium.

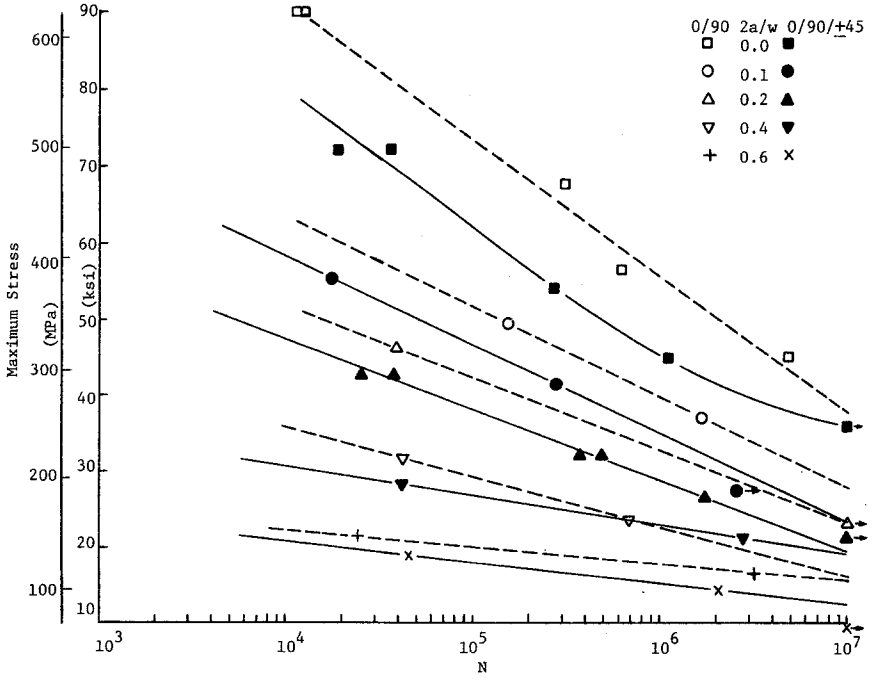

Figure 4 S–N curves for the unnotched and notched cross-plied boron–aluminium.

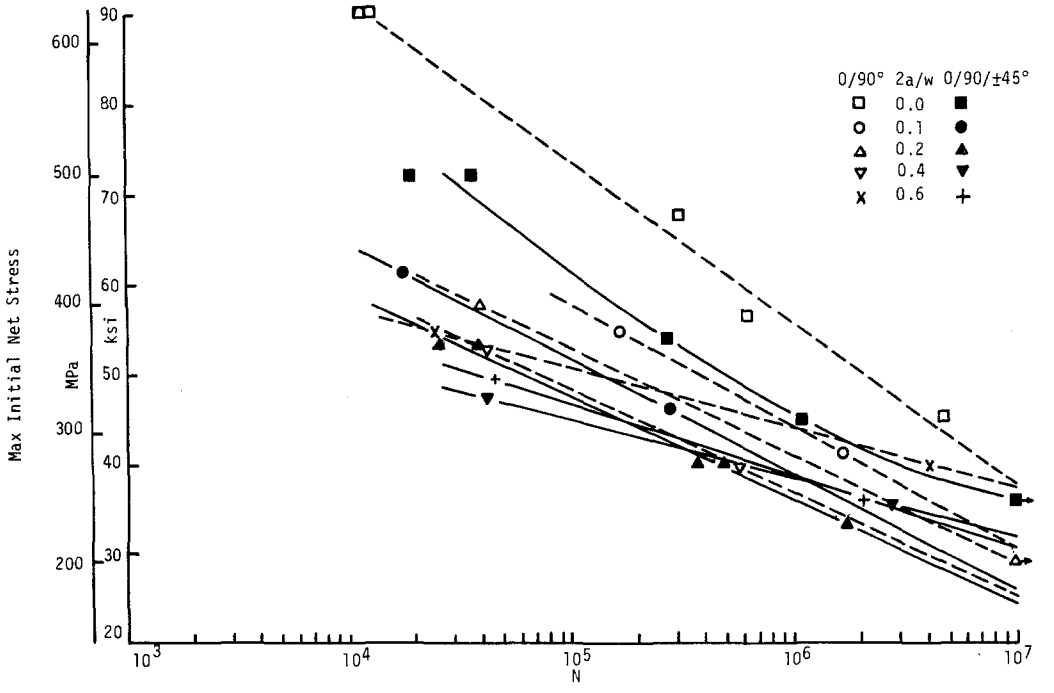

Figure 5 Initial net stress versus cycles to failure for the cross-plied boron–aluminium.

Fig. 3 shows the room temperature static tensile strengths plotted as a function of the ratio of notch length to specimen width. Critical values of the stress intensity factor, K_Q, were calculated by substituting the failure stress σ_{nom} and notch size, $2a$, into the expression:

$$K_Q = \sigma_{nom} (\pi a \sec \pi a/w)^{1/2}, \qquad (3)$$

where w is the specimen width. As can be observed, curves that pass reasonably close to the experimental points can be obtained by assuming K_Q values of about 36 MPa $m^{1/2}$ (33 x 10^3 psi $in.^{1/2}$) for the 0/90° and 33 MPa $m^{1/2}$ (30 x 10^3 psi $in.^{1/2}$) for the 0/90/± 45° material. Also shown in this figure is a curve of net failure stress calculated by substituting into Equation 3 σ_{net} $(w - 2a)/w$ for σ_{nom}. It is interesting to note that the net failure stress is expected to exhibit a minimum at a value of $2a/w$ of about 0.4.

The fatigue strengths exhibited by all of the room temperature specimens are shown in Fig. 4. The 10^7 cycle endurance limits, EL, for the unnotched materials were determined to be 248 MPa (36 x 10^3 psi) and 262 MPa (38 x 10^3 psi) for the 0/90° and 0/90/± 45° materials, respectively. The corresponding endurance ratios, EL/UTS, were 0.33 and 0.4. The presence of machined notches reduced the fatigue strengths of both materials. Larger cracks produced greater relative increases in the fatigue life. However, this effect was a maximum at $2a/w$ values of 0.4. Longer cracks then produced a decreasing effect. This phenomenon is seen more clearly in Fig. 5 in which the fatigue lives are expressed as a function of the net section stress amplitude. For both materials, progressively shorter lives were obtained at given net stress amplitudes from specimens containing cracks of increasing size up to a value of $2a/w$ of about 0.4. Longer lives were obtained from specimens containing cracks where $2a/w$ was greater than this value. This effect is similar to the maximum notch effect exhibited by statically

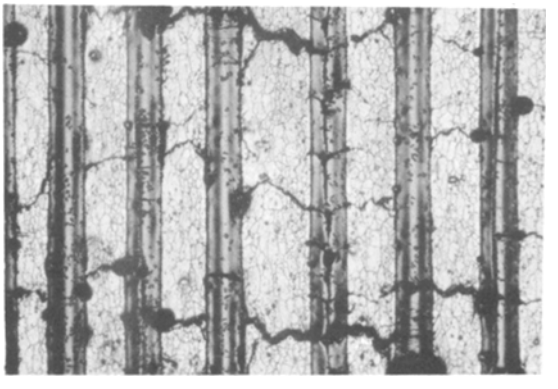

Figure 6 A 0° ply in a failed fatigue specimen (× 33).

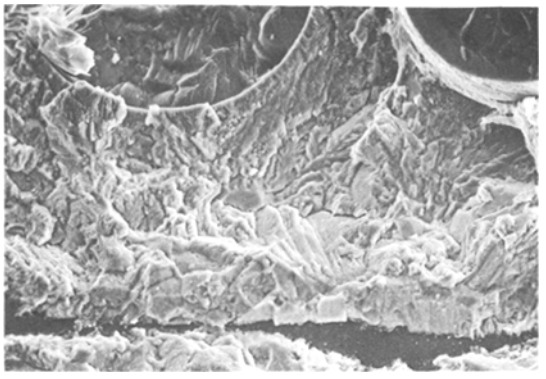

Figure 7 Tensile fracture surface of fatigued B–Al matrix (× 317).

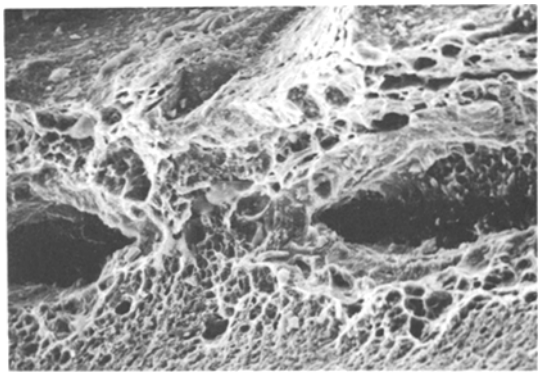

Figure 8 Tensile fracture surface of unfatigued B–Al matrix (× 710).

tested centre-notched specimens when expressed in terms of net stress. This has been discussed previously and, for a constant K_Q, occurs at $2a/w = 0.44$, as seen in Fig. 3.

Microscopic examination of the surface of fatigued specimens indicated that many cracks oriented perpendicular to the applied load were generated in the matrix. These cracks were present at the surface and throughout the body of the specimen. In some areas the cracks were observed to pass through fibres, although (as shown in Fig. 6) all of the matrix cracks were not necessarily connected with broken fibres. A fractographic examination indicated that the failed surface of a fatigued specimen contained many planar facets. A typical area such as that shown in Fig. 7 contrasted with the dimpled rupture appearance of the fracture surface of a statically failed specimen such as that shown in Fig. 8. Since an area similar in appearance to that shown in Fig. 8 was not observed on the fracture surface of fatigued specimens it was concluded that the fatigue crack had propagated completely through the matrix before failure of the fibres caused the composite to fail finally.

During fatigue cycling of notched specimens it was noted that the ends of the broken boron fibres tended to chip. This effect caused the surfaces of

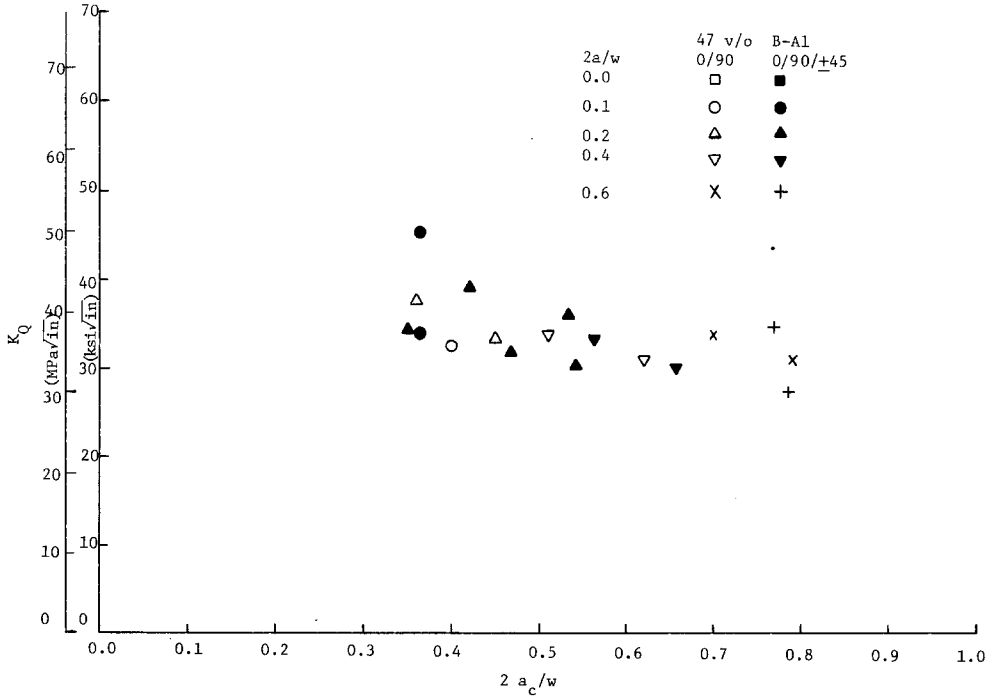

Figure 9 Fatigue failure stress intensity factors versus the failure crack length.

the propagating crack to become discoloured, and enabled the crack length at failure to be estimated. These computed crack lengths and the fatigue stress amplitudes were substituted into Equation 3 to give values of K_Q that would have been generated in the specimen during the final fatigue stress cycle. The results, shown in Fig. 9, indicate that failure of the notched fatigue specimens occurred at values of K_Q approximately the same as those obtained from static tests.

The effects of elevated temperatures on the fatigue strength of unnotched specimens is shown in Fig. 10. For the 0/90/±45° material, the fatigue strengths decreased about 20% as the test temperature was increased from room temperature to 200° C; a further decrease of about 10% was noted as the temperature was increased from 200 to 300° C. The endurance ratio decreased from the room temperature value of 0.40 to about 0.30 at 200° C and about 0.22 at 300° C For the 0/90° material there was relatively little change in the fatigue properties between room temperature and 200° C. In fact, the fatigue lives measured at 200° C were slightly greater at low values of the applied stress. At 300° C, however, a very large reduction in fatigue strength was obtained.

Microscopical examination indicated that the extensive matrix cracking exhibited by the specimens tested at room temperature also occurred in the matrix of specimens tested at elevated temperature. Discoloration of the fatigue crack surfaces also occurred and extensive shear of the matrix and fibre pull-out was exhibited.

The fatigue life data obtained at 300° C from the 0/90° or 0/90/±45° material are shown in Figs. 11 and 12. The superiority of the fatigue properties of the 0/90° material when tested at lower temperatures is not apparent when comparing the data included in these figures. The similarity of the properties is also confirmed when the fatigue lives are expressed in terms of the maximum applied net stress. These curves, shown in Figs. 13 and 14 also indicate that, when the applied stress is expressed in this manner, the fatigue properties become independent of initial crack length. Therefore it can be concluded that the stress-concentrating effect of a crack at 300° C is effectively zero. Thus, any attempt to describe

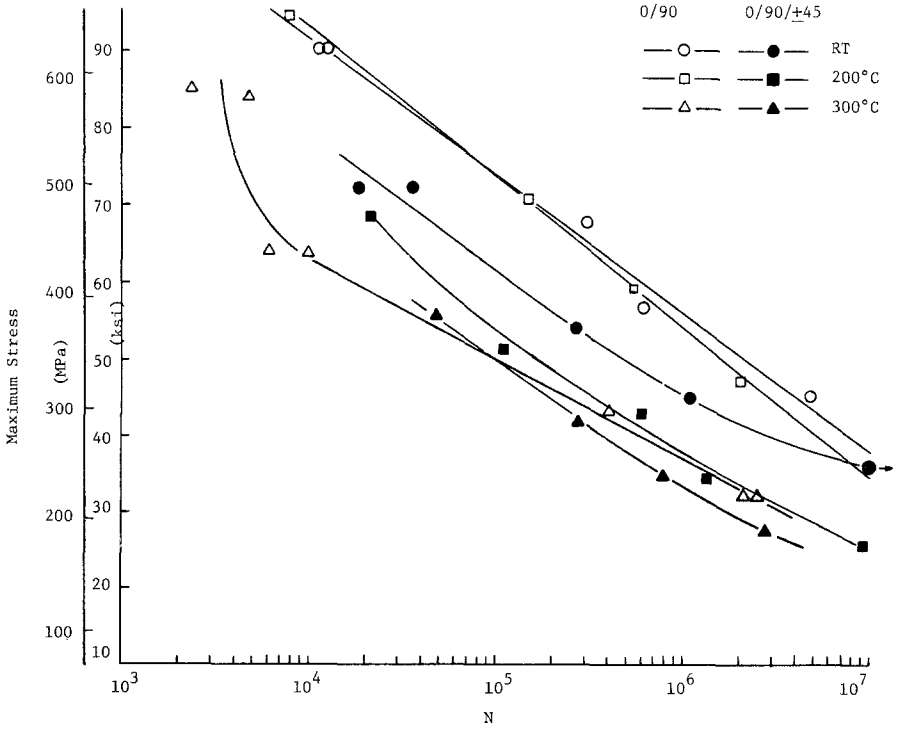

Figure 10 Effect of temperature on the fatigue behaviour of cross-plied boron–aluminium.

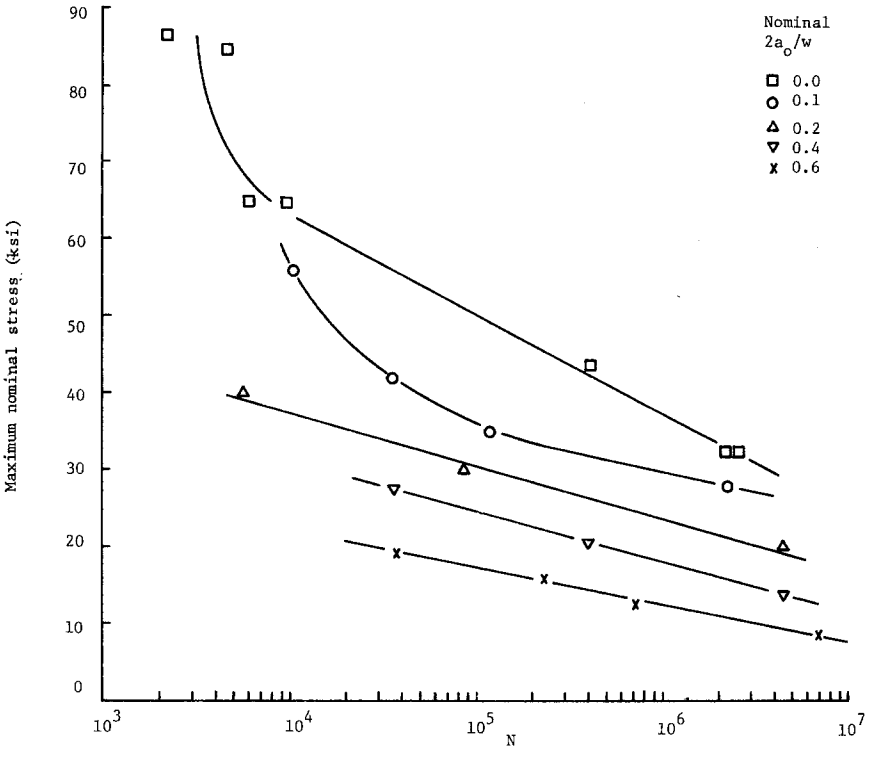

Figure 11 S–N curves for 0/90° 47B–6061 F Al fatigued at 300° C and $R = -1$.

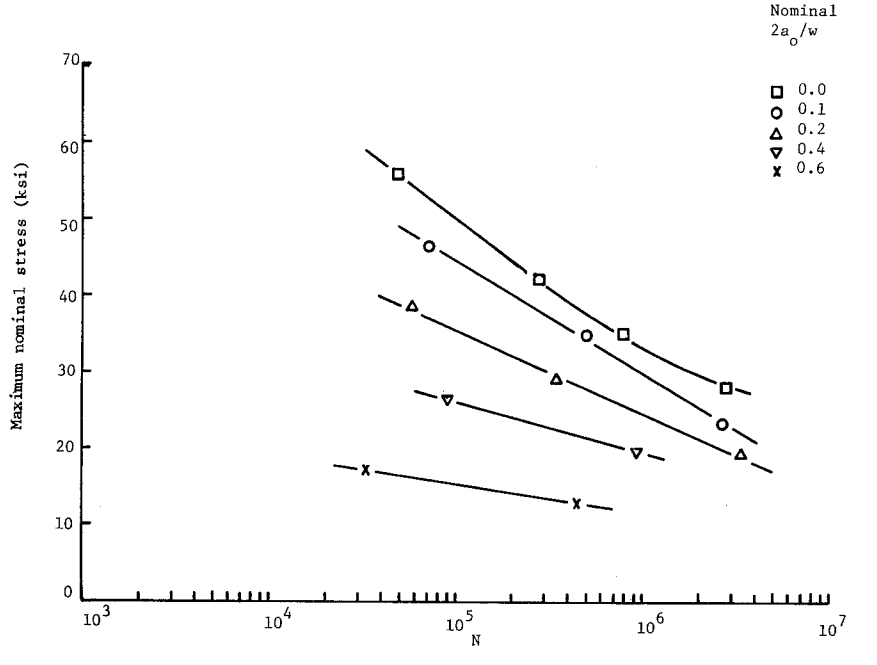

Figure 12 S–N curves for 0/90/± 45° 47B–6061 F Al fatigued at 300° C and $R = -1$.

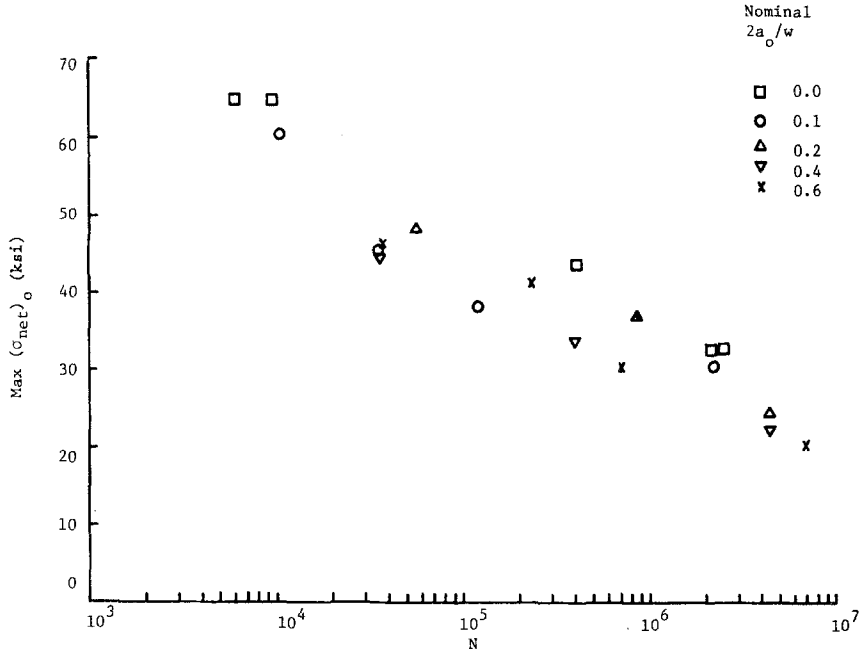

Figure 13 Initial net stress amplitude ($R = -1$) versus cyles to failure for 0/90° 47B–6061 F Al at 300° C.

the failure in terms of fracture mechanics principles would be inappropriate.

4. Conclusions

(1) Fatigue failure of cross-plied, 0/90° and 0/90/±45° boron–aluminium fibre composites occurs by the generation of multiple cracks in the matrix which precedes failure of the reinforcements.

(2) For the centre-notched specimen geometry the room temperature tensile and fatigue strength values appeared to be described in terms of a critical stress intensity. The elevated temperature values did not.

Acknowledgements

The authors wish to acknowledge the continued support and encouragement of Dr B. A. MacDonald.

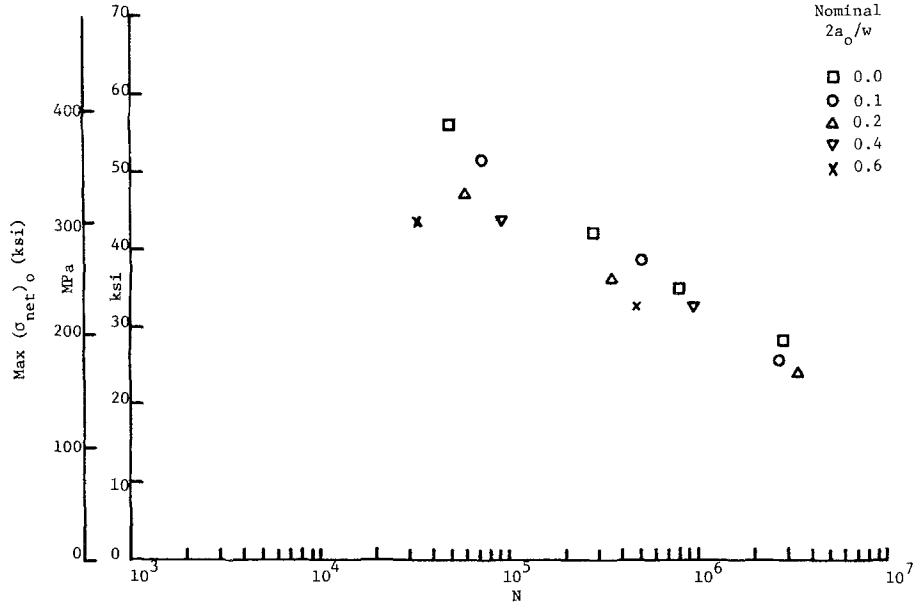

Figure 14 Initial net stress amplitude $R = -1$ versus cycles to failure for 0/90/± 45° 47B–6061 F Al at 300° C.

Financial support for the investigation was provided by the Office of Naval Research under contract number N00014-75-C-0352.

References

1. G. D. MENKE and I. J. TOTH, AFML-TR-71-102 (1971).
2. R. HANCOCK, ASTM STP 497 (1972) 483.
3. K. G. KREIDER and K. M. PREWO, "Metal Matrix Composites", Vol 4, edited by K. G. Kreider (Academic Press, London, 1974) p. 399.
4. J. R. KERR, J. F. HASKINS and B. A. STEIN, ASTM STP 602, Vol. 3 (1976).
5. M. A. WRIGHT and D. WELCH, *J. Fiber Sci. and Tech.* in press.
6. C. T. SUN and K. M. PREWO, *J. Comp. Mats.* **10** (1977) 164.
7. J. L. CHRISTIAN, Proceedings of the International Conference on Composite Materials, Geneva-Boston, (1975) p. 706.
8. H.W. HERRING NASA Rep. No. TND-3202 (1966).
9. M. A. WRIGHT and J. L. WILLS, *J. Mech. Phys. Solids* **22** (1974) 161.

Received 17 May and accepted 19 July 1978.